Fast microwave-driven three-qubit gates for cavity-coupled superconducting qubits

Edwin Barnes,[1] Christian Arenz,[2] Alexander Pitchford,[3] and Sophia E. Economou[1,*]
[1]*Department of Physics, Virginia Tech, Blacksburg, Virginia 24061, USA*
[2]*Department of Chemistry, Princeton University, Princeton, New Jersey 08544, USA*
[3]*Department of Physics, Aberystwyth University, Aberystwyth, United Kingdom*
(Received 29 December 2016; published 6 July 2017)

Although single- and two-qubit gates are sufficient for universal quantum computation, single-shot three-qubit gates greatly simplify quantum error correction schemes and algorithms. We design fast, high-fidelity three-qubit entangling gates based on microwave pulses for transmon qubits coupled through a superconducting resonator. We show that when interqubit frequency differences are comparable to single-qubit anharmonicities, errors occur primarily through a single unwanted transition. This feature enables the design of fast three-qubit gates based on simple analytical pulse shapes that are engineered to minimize such errors. We show that a three-qubit CCZ gate can be performed in 260 ns with fidelities exceeding 99.38%, or 99.99% with numerical optimization.

DOI: 10.1103/PhysRevB.96.024504

I. INTRODUCTION

Quantum information processing is one of the most exciting and rapidly growing fields of modern science, in large part due to quantum algorithms, which promise exponential speedup in solving important problems. Quantum two-level systems (qubits) are the fundamental carriers of quantum information, and among the most promising of these are qubits based on superconducting circuits [1,2]. Such an architecture is attractive because of the mature circuit fabrication technology and the ability to couple qubits together via resonators to implement logic gates [3].

For universal quantum computing, a certain set of high-fidelity logic gates suffices to implement any algorithm; this set is comprised of single-qubit gates along with one maximally entangling two-qubit gate. Three-qubit gates, which play a prominent role in algorithms and quantum error correction codes [4], can be decomposed in terms of a sequence of single- and two-qubit gates [5]. A maximally entangling three-qubit control-control-Z (CCZ) gate (described below) is typically performed using seven single-qubit gates and six entangling two-qubit gates, as shown in Fig. 1. The large number of gates needed makes it natural to explore whether a direct, single-shot three-qubit gate is preferable in terms of speed and fidelity.

There are two ways to implement logic gates in superconducting qubit systems. One is via tuning of the energy levels, which brings states into and out of resonance. The other is via oscillating microwave fields that induce transitions between energy levels, which offers the advantage of less susceptibility to low-frequency noise. This is because system parameters can be held fixed at noise-insensitive plateaus, leading to coherence times that are up to an order of magnitude longer than those of frequency-tunable systems [6]. Both approaches face the challenge of spectral crowding, especially in the context of superconducting transmon qubits where each qubit is a weakly anharmonic oscillator out of which the two lowest levels are selected to encode information [7]. In the case of many qubits coupled together, there are a large number of closely spaced transitions that need to be avoided during quantum gate operations. Generically, a way to avoid unwanted transitions is to consider the time-energy uncertainty principle, which tells us to make the operations slow. In realistic systems, however, this is not an option, as we need to perform operations at a time scale that is much faster than decay and decoherence.

There has been substantial theoretical effort to design pulses that avoid unwanted dynamics due to "harmful" transitions. A protocol that avoids leakage in single-qubit gates called DRAG has been introduced [8–12] and experimentally used [13,14]. For two-qubit gates, various approaches have been developed both for microwave drive [3,15–23] and for tuning [24–31]. In general, techniques developed in the context of one- or two-qubit gates are not directly applicable to three-qubit gates. Over the last few years, researchers have used numerical optimal control theory (OCT) techniques to design three-qubit gates [32–35]. Thus far, only tuning-based three-qubit gates have been demonstrated experimentally [4,36,37]. Although many experimental groups are pursuing an all-microwave-control approach, microwave-based three-qubit gates have yet to be implemented in the laboratory, most likely because there does not yet exist a simple protocol for them.

In this paper, we present an analytical protocol for a fast, high-fidelity three-qubit gate based on a single microwave pulse. The paper is organized as follows. In Sec. II, we show that by choosing qubit anharmonicities to be comparable to interqubit detunings, the spectrum resembles that of two qubits. In this regime, we can adapt a two-qubit gate protocol that two of us have recently developed [23], known as SWIPHT, to implement a microwave-driven three-qubit gate, locally equivalent to CCZ, in 260 ns. We show that such a fast gate can be achieved with fidelity exceeding 99.38% by using a hyperbolic secant pulse, which is smooth and experimentally simple to generate [38]. In Sec. III, we further show that our analytical solution can be successfully used as a starting point in OCT algorithms. The OCT solution reduces the infidelity by almost two orders of magnitude, pushing the gate fidelity to more than 99.99% without affecting the total gate duration, but at the cost of a more complicated pulse. In the same section, we also explore and characterize the robustness of the three-qubit gate based on the sech pulse, as well as the ones that come out

*economou@vt.edu

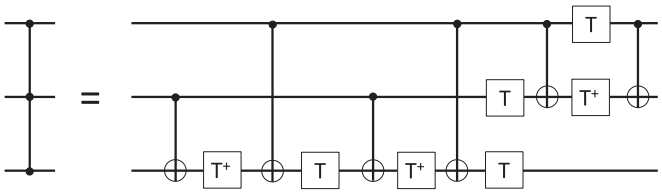

FIG. 1. Circuit diagram decomposition of the three-qubit CCZ gate in terms of seven single-qubit phase gates ($\top$) and six two-qubit CNOT gates.

of OCT and show that all of them are remarkably robust with respect to parameter uncertainties and fluctuations. Finally, we summarize our results and conclusions in Sec. IV.

II. CCZ GATE DESIGN

The most well-known three-qubit gate is the Toffoli gate, which is a NOT operation on one qubit conditional on the state of the other two qubits. It is equivalent to a CCZ gate, which amounts to a Z gate (a π rotation about the z axis) on one of the qubits conditional on the state of the other two qubits. In the computational basis, the CCZ gate is a diagonal matrix with a single diagonal element equal to -1, and the rest equal to 1.

The Hamiltonian describing the three-qubit–cavity system is

$$H_0 = \omega_c a^\dagger a + \sum_{\ell=1}^{3}\Big[\omega_\ell b_\ell^\dagger b_\ell + \frac{\alpha_\ell}{2} b_\ell^\dagger b_\ell (b_\ell^\dagger b_\ell - 1) + g_\ell (a^\dagger b_\ell + a b_\ell^\dagger)\Big]. \quad (1)$$

Here, $a^\dagger$ (a), $b_\ell^\dagger$ (b_ℓ) are creation (annihilation) operators for the cavity and the transmons, respectively, ω_ℓ denotes the energy splittings between the first excited state and ground state for each transmon, α_ℓ are the qubit anharmonicities, and g_ℓ are the coupling strengths between each transmon and the cavity. We denote the noninteracting ($g_\ell = 0$), "bare" eigenstates by $|n;ijk\rangle$, where $i,j,k = 0,1,\ldots$ label the individual transmon states, and where $n = 0,1,\ldots$ specifies the number of cavity photons. The eigenstates of the full, interacting system described by H_0 are denoted by $|\widetilde{n;ijk}\rangle$. When the qubits are detuned from each other and from the cavity, a common situation for superconducting qubits, and for typical qubit-cavity coupling strengths on the order of tens or hundreds of MHz, each dressed eigenstate has a large overlap with one bare state. Accordingly, the energies of the eigenstates are shifted slightly from those of the bare states they originate from. Thus, we use bare state labels n,i,j,k to label each interacting, dressed eigenstate according to the bare state with which it has the largest overlap. We define our computational states to be the lowest eight dressed states with zero cavity photons: $|\widetilde{ijk}\rangle$, with $i,j,k = 0,1$. We omit the cavity label when it is zero.

We focus on the case in which only one transmon is driven, and we take this to be transmon $\ell = 3$. In this case, the full Hamiltonian with driving included is

$$H(t) = H_0 + b_3\Omega(t)e^{i\omega_p t} + b_3^\dagger\Omega(t)e^{-i\omega_p t}, \quad (2)$$

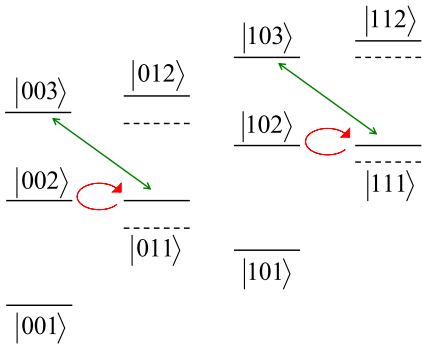

FIG. 2. Subsector of the three-qubit bare state spectrum that is relevant when the $|1\rangle\leftrightarrow|2\rangle$ transition of transmon 3 is driven. For generic parameters (dashed levels), there are four nearly degenerate transitions corresponding to the four logical states of transmons 1 and 2. When the anharmonicity is close to the detuning between transmons 2 and 3 (solid levels), $|011\rangle$ and $|002\rangle$ become nearly degenerate and mix strongly, as do $|111\rangle$ and $|102\rangle$, enabling two nearly degenerate two-qubit-like transitions $|\widetilde{011}\rangle\leftrightarrow|\widetilde{003}\rangle$ and $|\widetilde{111}\rangle\leftrightarrow|\widetilde{103}\rangle$ (green arrows). Dressed state tildes have been suppressed for clarity.

where $\Omega(t)$ and ω_p are the pulse envelope and frequency, respectively. The diagonal nature of the CCZ gate immediately points to transitionless evolution, i.e., evolution generated by pulses that transfer population between energy eigenstates only transiently and induce phases on the eigenstates. There is a fundamental challenge in inducing a minus sign to only one of the eigenstates while not affecting the remaining ones as needed for the CCZ gate, and it is related to the generic structure of a three-qubit system. The minus sign can be acquired by appropriately driving a single "target" transition that connects one computational state with an eigenstate outside the computational subspace. However, it is clear that when we drive one of the three qubits, e.g., transition $|1\rangle\leftrightarrow|2\rangle$ of qubit 3, there are four transitions that are near degenerate: $|\widetilde{ij1}\rangle\leftrightarrow|\widetilde{ij2}\rangle$, with i,j describing the 0,1 states of the other two qubits (see Fig. 2). If we attempt to implement the CCZ gate by simply selecting narrow-band pulses to resolve the target $|1\rangle\leftrightarrow|2\rangle$ transition of qubit 3 without disturbing the three remaining near-degenerate transitions, we will end up with extremely long pulses.

To speed up the pulse, we employ the SWIPHT method [23,39]. The main idea behind SWIPHT is to stop trying to avoid the nearly degenerate "harmful" transitions, but to instead purposely drive them using a pulse that is properly designed so that the net effect is that the driven states acquire trivial phases. This idea was utilized in Ref. [23] in the context of two cavity-coupled qubits, for which there are two near-degenerate transitions, to implement both the CNOT and the CZ gate. In the case of the CZ gate, which is the two-qubit analog of our three-qubit CCZ gate, a hyperbolic secant-shaped pulse was used, which yields an analytically solvable Schrödinger equation [40] for a two-level system. The fact that in the two-qubit case there are two transitions driven simultaneously in a prescribed way allowed us to tune two parameters, the detuning and bandwidth, to induce the correct phases on each eigenstate [41–43].

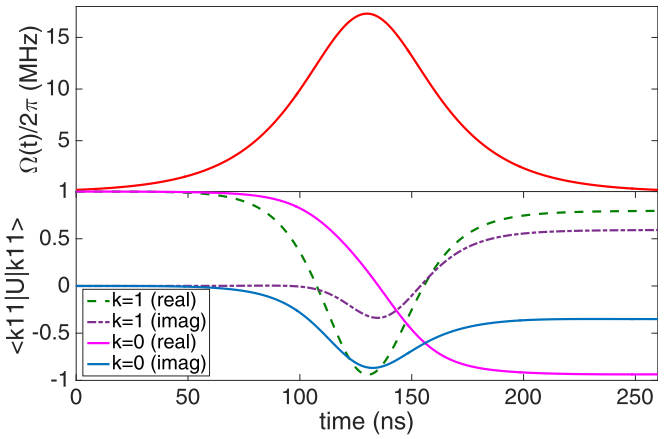

FIG. 3. Upper panel: the hyperbolic secant pulse $\Omega(t) = \Omega_0 \mathrm{sech}[\sigma(t-T/2)]$ used to perform the CCZ gate. Here, $\sigma = \delta/\sqrt{3} = 2\pi \times 6.12$ MHz, $T = 260.02$ ns, $\Omega_0 = 2\sigma/d = 2\pi \times 17.3$ MHz, and $d = 0.7074$ is the ratio of the dipole moments of the noninteracting single-qubit $|0\rangle \leftrightarrow |1\rangle$ transition and interacting harmful transition. This choice of Ω_0 implements a 4π rotation on the harmful transition. The simulations were performed using the following parameters (in GHz): $\omega_1 = 6.2$, $\omega_2 = 6.6$, $\omega_3 = 7.0$, $\omega_c = 7.15$, $\alpha_\ell = 0.35$, g_ℓ=0.13. Lower panel: simulation of the evolution operator matrix elements corresponding to the logical states involved in the target ($k = 0$) and harmful ($k = 1$) transitions. The target state $|\widetilde{011}\rangle$ picks up a π phase, while the state $|\widetilde{111}\rangle$ picks up a trivial 2π phase. Deviations from the ideal behavior are largely due to correctable local operations.

The protocol of Ref. [23] cannot be used straightforwardly due to the existence of the four $|\widetilde{ij1}\rangle \leftrightarrow |\widetilde{ij2}\rangle$ transitions: the number of pulse parameters is simply less than the number of constraints. We address this issue by taking a second look at the spectrum to explore whether a more advantageous structure can be achieved by appropriately choosing the static parameters, i.e., the qubit and cavity frequencies, the anharmonicity, and the coupling strength. (We begin by assuming the latter two are the same for all qubits, although this assumption will be lifted later.) Out of the four transitions $|\widetilde{ij1}\rangle \leftrightarrow |\widetilde{ij2}\rangle$, we aim to isolate only two near-degenerate ones so that the spectrum will resemble the two-qubit spectrum, which we know how to control. If we choose the frequency of the qubits to differ approximately by the anharmonicity, then the bare state $|011\rangle$ is degenerate with $|002\rangle$ and $|111\rangle$ is degenerate with $|102\rangle$, which means that the two states $|011\rangle$ and $|111\rangle$ will mix more strongly with the excited states $|002\rangle$ and $|102\rangle$. As a result, when the third transmon qubit is driven, there will be a significant dipole matrix element between the states $|\widetilde{011}\rangle$ and $|\widetilde{003}\rangle$ and between the states $|\widetilde{111}\rangle$ and $|\widetilde{103}\rangle$. Transitions near these frequencies involving the remaining two states, $|\widetilde{001}\rangle$ and $|\widetilde{101}\rangle$, will not be present (see Fig. 2). This is analogous to the spectrum engineering used for the two-qubit MAP gate [21].

With this spectrum, we are now able to adapt the SWIPHT protocol. We choose the two transitions $|\widetilde{011}\rangle \leftrightarrow |\widetilde{003}\rangle$ and $|\widetilde{111}\rangle \leftrightarrow |\widetilde{103}\rangle$ as the target and the harmful transitions, respectively. We select a hyperbolic secant pulse of area 4π, which acts on both transitions simultaneously (see Fig. 3). Applying this pulse resonantly to the harmful transition will drive it strongly, but will only induce a trivial phase of 2π on it. This result is independent of the pulse bandwidth σ, which is a free parameter that we can adjust to ensure that the phase acquired by the target transition is -1 as needed for the CCZ gate. The analyticity of the solution leads to an explicit result for this phase: $\phi = 2\arctan(4\delta\sigma/[\delta^2 - 3\sigma^2])$, where δ is the detuning between the two transitions [43]. The value of the bandwidth that achieves $\phi = \pi$ is $\sigma = \delta/\sqrt{3}$.

III. NUMERICAL SIMULATIONS TO CHARACTERIZE GATE PERFORMANCE

So far, our discussion ignores the rest of the Hilbert space and assumes that the presence of the large number of states and transitions not directly involved in our protocol will not affect our result. We now test this with simulations of the full, realistic system. The system and pulse parameters we use are shown in the caption of Fig. 3. The pulse envelope is shown in the upper panel, where it can be seen that the total duration is $T = 260$ ns. We retain enough states out of the infinite Hilbert space to ensure that the results converge, which amounts to keeping four cavity states and five states for each of the qubits, resulting in a 500-dimensional Hilbert space. The matrix elements of the evolution operator corresponding to the logical states involved in the target and harmful transitions are shown in the lower panel of Fig. 3. Although deviations from the ideal values $\langle 011|U(T)|011\rangle = -1$ and $\langle 111|U(T)|111\rangle = 1$ are evident, we will see that these deviations are largely due to the pulse generating additional local operations that can be corrected with single-qubit gates.

A. Fidelity and robustness of sech pulse

We quantify the performance of our CCZ gate using the fidelity defined in Ref. [44], $F = \frac{1}{72}[\mathrm{Tr}(MM^\dagger) + |\mathrm{Tr}(M)|^2]$, where $M = U_{\mathrm{ideal}}U^\dagger$, U is the actual evolution operator truncated to the three-qubit logical subspace, and U_{ideal} is the target gate operation. To account for possible local operations, we choose U_{ideal} to be a generalized CCZ gate which is locally equivalent to the standard CCZ up to single-qubit phase gates and a global phase: $U_{\mathrm{ideal}} = e^{-i\phi_0 - i\sum_j \phi_j \sigma_{j,z}}\mathrm{diag}(1,1,1,-1,1,1,1,1)$, and we maximize F over the phases ϕ_k. We find that our gate has a fidelity of $F = 0.993\,881$ with phases $\phi_0 = 1.191\,87$, $\phi_1 = 0.036\,07$, $\phi_2 = -0.028\,42$, $\phi_3 = 0.190\,56$. Considering the complexity and spectral crowding of the Hilbert space and the simplicity of our pulse shape, this is a remarkable, and perhaps somewhat surprising, result. For comparison, even if it were possible to perform every single-qubit gate in the CCZ decomposition shown in Fig. 1 with 99.9% fidelity and every two-qubit gate with 99% fidelity (near the surface code fault-tolerant threshold [45]), the fidelity of the resulting CCZ gate would be ~93.5%, or ~95% using optimal decompositions [46,47], while the total duration would exceed a microsecond. We thus see that the SWIPHT method reduces the three-qubit gate infidelity by an order of magnitude while reducing the gate time by a factor of ~5.

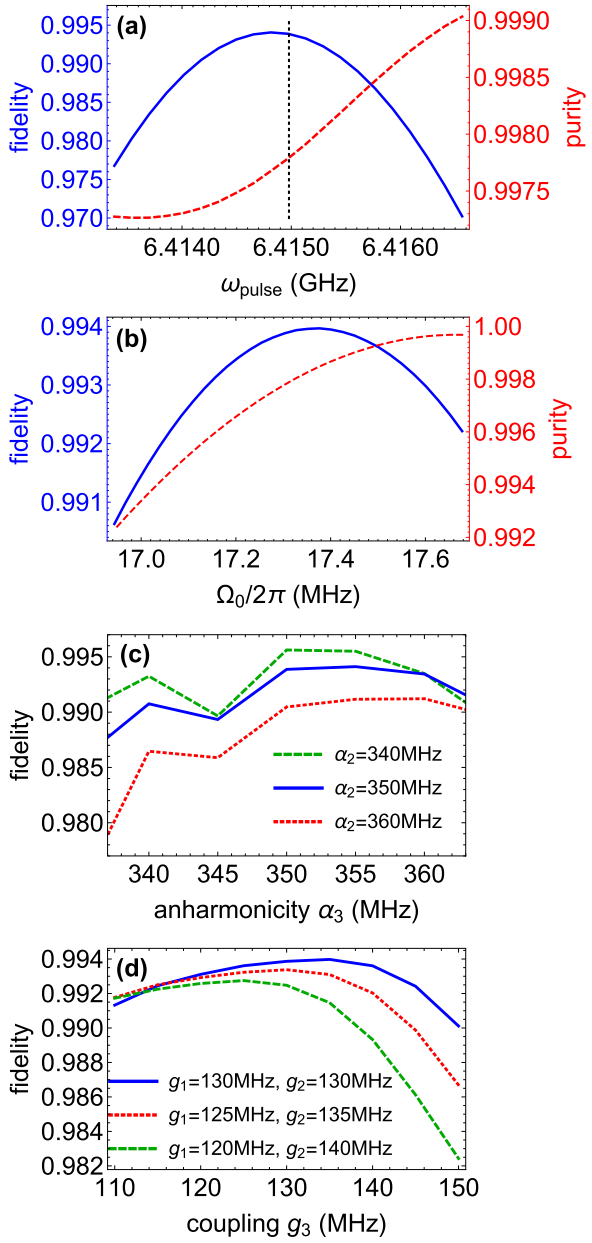

FIG. 4. (a), (b) Fidelity as a function of (a) pulse frequency and (b) pulse amplitude. The vertical dotted line in (a) indicates the frequency of the harmful transition. The purity is also included (red dashed, right scale) for comparison. (c), (d) Robustness of three-qubit SWIPHT gate to variations in anharmonicity and coupling strength. Parameters are as in Fig. 3 except as indicated.

The fidelity as a function of the pulse frequency and amplitude is shown in Figs. 4(a) and 4(b), where it is evident that the performance is insensitive to typical variations on the scale of 100s of kHz. The figure also shows the purity, which not only remains high despite the parameter variations, it actually increases with increasing pulse frequency and amplitude, indicating that most of the error is contained within the logical qubit subspace in these regimes. Figures 4(c) and 4(d) show that the fidelity is also insensitive to variations in system parameters at the level of several MHz. In addition to demonstrating robustness, these results show that still higher fidelities can be achieved by optimizing over pulse or system parameters.

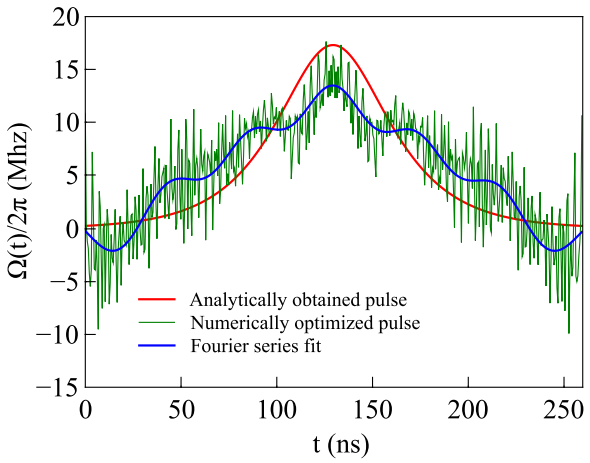

FIG. 5. Pulse envelope implementing the CCZ gate as a function of time. The smooth red curve shows the analytically obtained pulse corresponding to a fidelity of $F = 0.993\,881$. The rapidly modulated green curve shows the numerically optimized pulse using OCT, which further decreases the infidelity by two orders of magnitude ($F = 0.999\,941$). The more slowly modulated blue curve ("smoothed OCT") shows a Fourier series fit of the numerically optimized pulse with fidelity $F = 0.995\,574$.

B. Improving the fidelity via optimal control

We now address the issue of further increasing the gate fidelity via OCT by using our analytical pulse as a starting point. Here, we use the GRAPE algorithm [48] in QUTIP [49,50] in order to find the pulse $\Omega(t)$ that maximizes the fidelity. If we divide the total evolution time T into equispaced time intervals, $\Delta t = T/n$, on which $H(t)$ is assumed to be piecewise constant, the total evolution $U(T)$ can be written as a time-ordered product of unitary operators: $U(T) = \prod_{j=1}^{n} e^{-iH(t_j)\Delta t}$, where $t_j \in [(j-1)\Delta t, j\Delta t]$. Denoting by $\Omega_1, \ldots, \Omega_n$ the piecewise constant pulse amplitudes, it is straightforward to calculate the gradient of F with respect to Ω_i, noting that an expression for $\frac{\partial U(T)}{\partial \Omega_i}$ can be found in [51]. After having modified the gradient expression in [49,50] accordingly, we maximized F for a total evolution time $T = 260.06$ ns using $n = 500$ time slots and taking the generalized CCZ gate with preoptimized phases ϕ_k as the target gate.

The results are shown in Fig. 5. As an initial guess pulse we took the 4π hyperbolic secant pulse with $\sigma = \delta/\sqrt{3}$ (smooth red curve), which has the advantage of being already close to the optimal solution. The rapidly modulated (green) curve shows the optimized pulse corresponding to a fidelity of $F = 0.999\,941$ and the slowly modulated (blue) curve shows a Fourier series fit with seven coefficients yielding $F = 0.995\,574$. Thus, starting from the analytically obtained pulse, the use of OCT can further decrease the infidelity by a few orders of magnitude. We find that using simple, near-optimal analytical pulses as a seed in the numerical optimization algorithm can be dramatically more efficient than blind numerical searches. The fact that all three pulse shapes

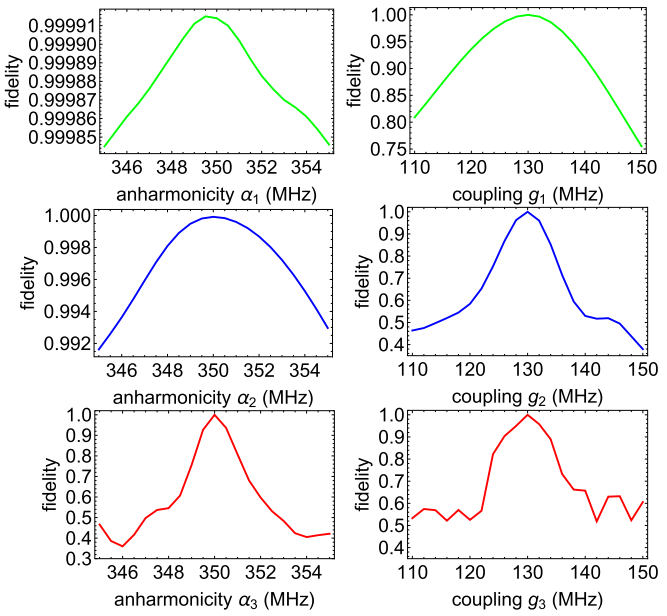

FIG. 6. Robustness of OCT pulse against variations in anharmonicity (left column) and in qubit-cavity coupling (right column) for each of the three qubits. All other parameters are as in Fig. 3.

shown in Fig. 5 implement high-fidelity CCZ gates shows that our scheme is not sensitive to pulse shape.

C. Robustness of gate to slow noise in system and pulse parameters

Since a particular condition for the system parameters has been assumed, it is natural to explore how robust our scheme

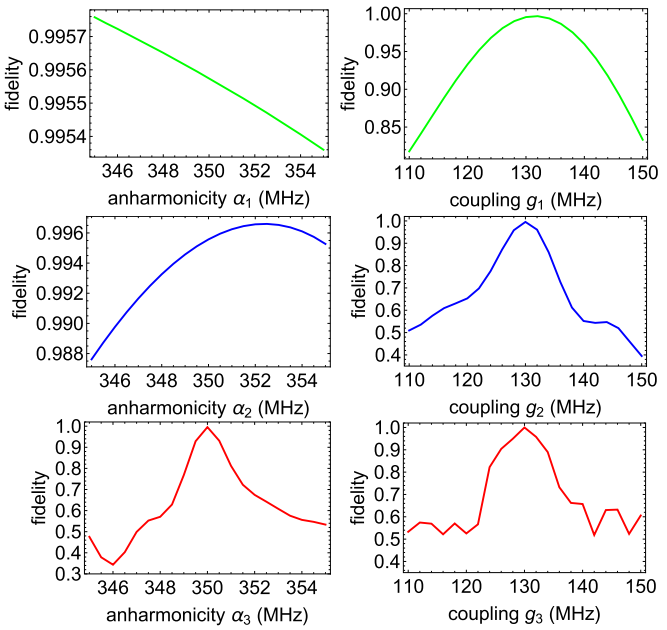

FIG. 7. Robustness of smoothed OCT pulse against variations in anharmonicity (left column) and in qubit-cavity coupling (right column) for each of the three qubits. All other parameters are as in Fig. 3.

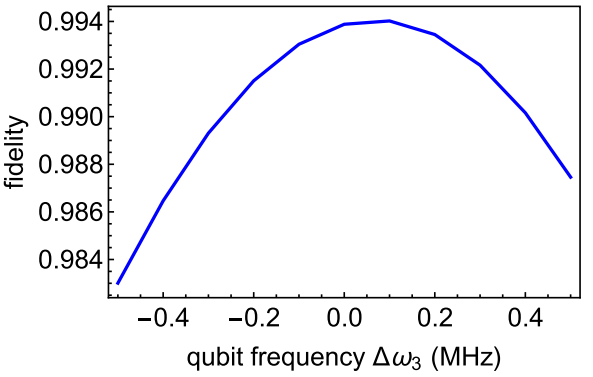

FIG. 8. Robustness of analytical sech pulse against variations in the frequency of the driven qubit.

is under variations or noise in these parameters. Figures 6 and 7 show the robustness of our OCT and smoothed OCT pulses (see Fig. 5) to noise in system parameters, including anharmonicities and qubit-cavity couplings. We consider the case of slow noise in which noise fluctuations are assumed

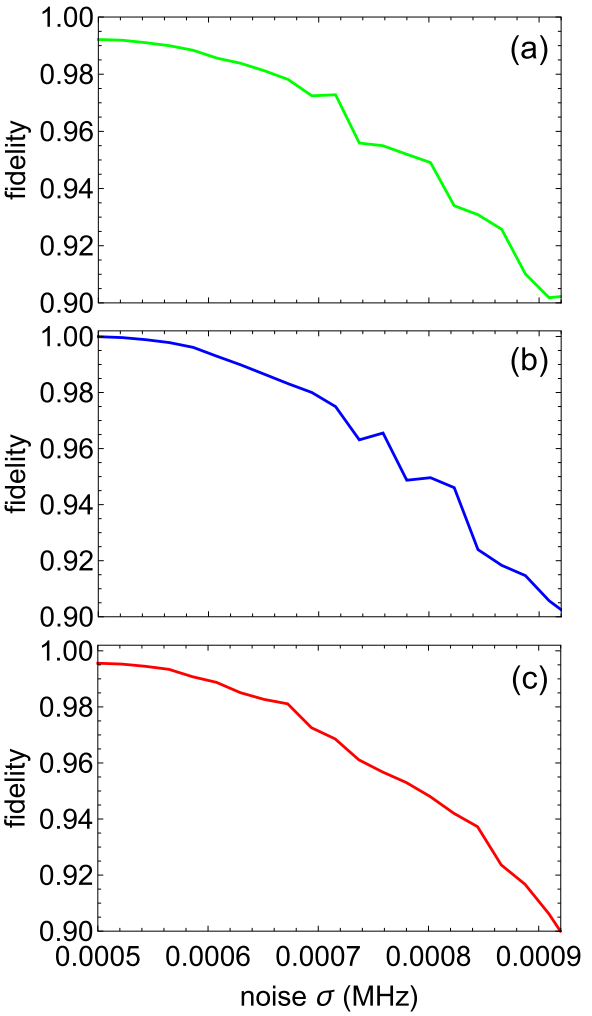

FIG. 9. Robustness of (a) analytical, (b) OCT, and (c) smoothed OCT pulse against high-frequency noise fluctuations in the pulse amplitude.

static over the duration of the gate. In this case, it suffices to look at the gate fidelity as a function of system parameters in order to estimate the effect of noise on the three-qubit gate fidelity. We see that the performance of the OCT and smoothed OCT pulses is largely insensitive to variations in system parameters associated with the qubits which are not driven (qubits 1 and 2), while it is more sensitive to variations in the driven qubit (qubit 3). Thus, the gate fidelity will be relatively insensitive to noise in the undriven qubits and more sensitive to noise in the driven qubit. This is in contrast to the analytical sech pulse (Fig. 3), which is significantly less sensitive to all system parameters, including those associated with the driven qubit [see Figs. 4(c) and 4(d)]. To further illustrate this point, we have also investigated the dependence of the gate fidelity for the analytical pulse on the frequency of the driven qubit, which is shown in Fig. 8. Here, it is evident that the fidelity remains above 99% even for fluctuations in the qubit frequency on the order of 200 kHz, which exceeds qubit energy linewidths in typical experiments. This demonstrates that the performance of our three-qubit gate is very good even in the presence of realistic noise levels. This is consistent with the robustness of two-qubit SWIPHT gates in the presence of realistic values of T_1, T_2 [39]; the reduction of gate times afforded by SWIPHT minimizes the impact of relaxation and decoherence.

In addition to system parameter noise, the pulse itself may also feature fluctuations. Figures 4(a) and 4(b) show that the analytical sech pulse (Fig. 3) is robust against slow fluctuations in the drive frequency and pulse amplitude. In the former case, we see that the fidelity remains above 99% for frequency fluctuations up to nearly 1 MHz, well above typical experimental variations on the order of 10 s to 100 kHz.

D. Robustness of gate to high-frequency noise in pulse amplitude

Figure 9 shows the performance of all three pulses (analytical, OCT, and smoothed OCT) in the presence of high-frequency noise in the pulse amplitude. In these simulations, each 0.5-ns segment of the pulse envelope is allowed to fluctuate independently according to a Gaussian distribution with standard deviation σ, corresponding to ultrafast noise acting on the scale of 2 GHz. The figure shows that even in the presence of such strong noise (well beyond typical experimental levels), fidelities remain above 90% for standard deviations up to nearly 1 kHz.

IV. SUMMARY AND CONCLUSIONS

We have designed a microwave-based single-shot three-qubit gate for transmon qubits generated by a simple, fast, and smooth pulse. Our gate is based on working in a regime where the spectrum is reminiscent of a two-qubit–cavity system and applying the SWIPHT method. Even without optimizing over parameters or pulse shape, the gate fidelity comfortably exceeds surface code thresholds by an order of magnitude while reducing the gate time by a factor of 5. We have demonstrated that using our analytical pulse as a starting point in optimal control theory leads to a further decrease in the gate infidelity by two orders of magnitude.

[1] J. Clarke and F. K. Wilhelm, Nature (London) **453**, 1031 (2008).
[2] M. H. Devoret and R. J. Schoelkopf, Science **339**, 1169 (2013).
[3] J. Majer, J. M. Chow, J. M. Gambetta, J. Koch, B. R. Johnson, J. A. Schreier, L. Frunzio, D. I. Schuster, A. A. Houck, A. Wallraff *et al.*, Nature (London) **449**, 443 (2007).
[4] M. D. Reed, L. DiCarlo, S. E. Nigg, L. Sun, L. Frunzio, S. M. Girvin, and R. J. Schoelkopf, Nature (London) **482**, 382 (2012).
[5] M. A. Nielsen and I. L. Chuang, *Quantum Computation and Quantum Information* (Cambridge University Press, Cambridge, England, 2000).
[6] C. Rigetti, J. M. Gambetta, S. Poletto, B. L. T. Plourde, J. M. Chow, A. D. Córcoles, J. A. Smolin, S. T. Merkel, J. R. Rozen, G. A. Keefe *et al.*, Phys. Rev. B **86**, 100506 (2012).
[7] J. Koch, T. M. Yu, J. Gambetta, A. A. Houck, D. I. Schuster, J. Majer, A. Blais, M. H. Devoret, S. M. Girvin, and R. J. Schoelkopf, Phys. Rev. A **76**, 042319 (2007).
[8] F. Motzoi, J. M. Gambetta, P. Rebentrost, and F. K. Wilhelm, Phys. Rev. Lett. **103**, 110501 (2009).
[9] A. M. Forney, S. R. Jackson, and F. W. Strauch, Phys. Rev. A **81**, 012306 (2010).
[10] J. M. Gambetta, F. Motzoi, S. T. Merkel, and F. K. Wilhelm, Phys. Rev. A **83**, 012308 (2011).
[11] F. Motzoi and F. K. Wilhelm, Phys. Rev. A **88**, 062318 (2013).
[12] R. Schutjens, F. A. Dagga, D. J. Egger, and F. K. Wilhelm, Phys. Rev. A **88**, 052330 (2013).
[13] J. M. Chow, L. DiCarlo, J. M. Gambetta, F. Motzoi, L. Frunzio, S. M. Girvin, and R. J. Schoelkopf, Phys. Rev. A **82**, 040305(R) (2010).
[14] Z. Chen, J. Kelly, C. Quintana, R. Barends, B. Campbell, Y. Chen, B. Chiaro, A. Dunsworth, A. G. Fowler, E. Lucero *et al.*, Phys. Rev. Lett. **116**, 020501 (2016).
[15] J. Li, K. Chalapat, and G. S. Paraoanu, Phys. Rev. B **78**, 064503 (2008).
[16] W. R. Kelly, Z. Dutton, J. Schlafer, B. Mookerji, T. A. Ohki, J. S. Kline, and D. P. Pappas, Phys. Rev. Lett. **104**, 163601 (2010).
[17] C. Rigetti and M. Devoret, Phys. Rev. B **81**, 134507 (2010).
[18] C.-P. Yang, S.-B. Zheng, and F. Nori, Phys. Rev. A **82**, 062326 (2010).
[19] Z. Kim, B. Suri, V. Zaretskey, S. Novikov, K. D. Osborn, A. Mizel, F. C. Wellstood, and B. S. Palmer, Phys. Rev. Lett. **106**, 120501 (2011).
[20] J. M. Chow, J. M. Gambetta, A. D. Córcoles, S. T. Merkel, J. A. Smolin, C. Rigetti, S. Poletto, G. A. Keefe, M. B. Rothwell, J. R. Rozen *et al.*, Phys. Rev. Lett. **109**, 060501 (2012).
[21] J. M. Chow, J. M. Gambetta, A. W. Cross, S. T. Merkel, C. Rigetti, and M. Steffen, New J. Phys. **15**, 115012 (2013).
[22] J. M. Chow, J. M. Gambetta, E. Magesan, D. W. Abraham, A. W. Cross, B. R. Johnson, N. A. Masluk, C. A. Ryan, J. A. Smolin, S. J. Srinivasan *et al.*, Nat. Commun. **5**, 4015 (2014).
[23] S. E. Economou and E. Barnes, Phys. Rev. B **91**, 161405(R) (2015).

[24] F. W. Strauch, P. R. Johnson, A. J. Dragt, C. J. Lobb, J. R. Anderson, and F. C. Wellstood, Phys. Rev. Lett. **91**, 167005 (2003).
[25] L. DiCarlo, J. M. Chow, J. M. Gambetta, L. S. Bishop, B. R. Johnson, D. I. Schuster, J. Majer, A. Blais, L. Frunzio, S. M. Girvin *et al.*, Nature (London) **460**, 240 (2009).
[26] L. DiCarlo, M. D. Reed, L. Sun, B. R. Johnson, J. M. Chow, J. M. Gambetta, L. Frunzio, S. M. Girvin, M. H. Devoret, and R. J. Schoelkopf, Nature (London) **467**, 574 (2010).
[27] E. Lucero, R. Barends, Y. Chen, J. Kelly, M. Mariantoni, A. Megrant, P. O'Malley, D. Sank, A. Vainsencher, J. Wenner *et al.*, Nat. Phys. **8**, 719 (2012).
[28] J. Ghosh, A. Galiautdinov, Z. Zhou, A. N. Korotkov, J. M. Martinis, and M. R. Geller, Phys. Rev. A **87**, 022309 (2013).
[29] D. J. Egger and F. K. Wilhelm, Supercond. Sci. Technol. **27**, 014001 (2014).
[30] J. M. Martinis and M. R. Geller, Phys. Rev. A **90**, 022307 (2014).
[31] R. Barends, J. Kelly, A. Megrant, A. Veitia, D. Sank, E. Jeffrey, T. C. White, J. Mutus, A. G. Fowler, B. Campbell *et al.*, Nature (London) **508**, 500 (2014).
[32] V. M. Stojanović, A. Fedorov, A. Wallraff, and C. Bruder, Phys. Rev. B **85**, 054504 (2012).
[33] E. Zahedinejad, J. Ghosh, and B. C. Sanders, Phys. Rev. Lett. **114**, 200502 (2015).
[34] E. Zahedinejad, J. Ghosh, and B. C. Sanders, Phys. Rev. Appl. **6**, 054005 (2016).
[35] J. K. Moqadam, R. Portugal, N. F. Svaiter, and G. de Oliveira Corrêa, Phys. Rev. A **87**, 042324 (2013).
[36] A. Fedorov, L. Steffen, M. Baur, M. P. da Silva, and A. Wallraff, Nature (London) **481**, 170 (2012).
[37] M. Mariantoni, H. Wang, T. Yamamoto, M. Neeley, R. C. Bialczak, Y. Chen, M. Lenander, E. Lucero, A. D. O'Connell, D. Sank *et al.*, Science **334**, 61 (2011).
[38] H. S. Ku, J. L. Long, X. Wu, M. Bal, R. E. Lake, E. Barnes, S. E. Economou, and D. P. Pappas, arXiv:1704.00803.
[39] X.-H. Deng, E. Barnes, and S. E. Economou, arXiv:1703.03514.
[40] N. Rosen and C. Zener, Phys. Rev. **40**, 502 (1932).
[41] S. E. Economou, L. J. Sham, Y. Wu, and D. G. Steel, Phys. Rev. B **74**, 205415 (2006).
[42] S. E. Economou and T. L. Reinecke, Phys. Rev. Lett. **99**, 217401 (2007).
[43] S. E. Economou, Phys. Rev. B **85**, 241401(R) (2012).
[44] L. H. Pedersen, N. M. Møller, and K. Mølmer, Phys. Lett. A **367**, 47 (2007).
[45] A. G. Fowler, M. Mariantoni, J. M. Martinis, and A. N. Cleland, Phys. Rev. A **86**, 032324 (2012).
[46] V. V. Shende and I. L. Markov, Quantum Inf. Comput. **9**, 461 (2009).
[47] N. Yu and M. Ying, arXiv:1301.3727.
[48] N. Khaneja, T. Reiss, C. Kehlet, T. Schulte-Herbrüggen, and S. J. Glaser, J. Magn. Reson. **172**, 296 (2005).
[49] J. Johansson, P. Nation, and F. Nori, Comput. Phys. Commun. **183**, 1760 (2012).
[50] R. Johansson, P. Nation, A. Pitchford, C. Granade, A. L. Grimsmo, markusbaden, A. Vardhan, P. Migda, kafischer, D. Vasilyev *et al.*, qutip/qutip: Qutip-4.0.0 (2016), https://doi.org/10.5281/zenodo.220867
[51] R. Nigmatullin and S. G. Schirmer, New J. Phys. **11**, 105032 (2009).